

## Research Article

### Joint use of Bond Graph Approach and Scattering Formalism for an Electrical Modeling of Patch Antenna Array

<sup>1</sup>Hichem Taghouti, <sup>1</sup>Sabri Jmal and <sup>1,2</sup>Abdelkader Mami

<sup>1</sup>Department of Electrical Engineering, Laboratory of Analysis and Control Systems, ENIT-BP 37, 1002 Tunis Le BELVEDERE,

<sup>2</sup>Department of Physics, Faculty of Sciences of Tunis, Laboratory of High Frequency, Electronic Circuits and Systems, University Campus 2092-Tunis El Manar, Tunisia

**Abstract:** In this study we present another joint application of the bond graph approach and the scattering formalism for an electrical modeling of a patch antenna array. First, the aim of our application is to build the overall bond graph model of the antenna array using the first principle (physical interpretation to bond graph word of a physical system) of the developed technique by our research team. Second, the simplified model, performed on the found conventional bond graph model gives us easily, on the one hand, the scattering matrix  $S_{ij}$  (applying the analytical operating procedure); on the other hand, the electrical model of the patch antenna array. The proposed technique is validated by a comparative study between the simulations of the scattering parameters  $S_{ij}$  of the studied structure and the simulations of those founded directly from the electrical model of the antenna. In this study we recall that, the used networks patch antenna has multi-triangular and geometric structures.

**Keywords:** Bond graph modeling, lumped elements, multi-triangular structure, patch antenna array, scattering bond graph approach, RF and microwave circuits

## INTRODUCTION

The communication wireless systems which has a micro strip structure was the origin of the development printed antennas (patch antenna laminated antennas) (Ferchichi *et al.*, 2009) which are often used in networks to improve performance and enable the realization of very special functions. Typically, micro strip or patch antenna is an antenna which is better than other antennas. It is light, cheap and easy to integrate with electronic equipment (Galehdar *et al.*, 2007). The rectangular, multi-triangular, circular and rectilinear patch has been widely used in a variety of antenna array (Mehouachi *et al.*, 2014).

In fact, they are the interface between the transmission and reception block (Pozart, 1998). Following the wide varieties of communication systems, the choice of type of antenna, the parameters studied and the study tool vary from one application to another. For these reasons, the choice of tools for modeling and simulation is very important.

Indeed, many study skills antennas have evolved according to the requirements of modern applications (Mekki, 2004). These techniques can be classified according to their principles; some are based on purely

numerical methods and the other on analytical approximations (Su *et al.*, 2004).

In this study, the analytical method used is developed by Taghouti and Mami (2009) where they used, jointly, the bond graph approach (Kamel and Dauphin-Tanguy, 1993) and the Scattering formalism (Paynter *et al.*, 1988) for the electrical modeling of patch antennas with different structures.

At the first part of this study, we present the basics of the physical analysis method for the modeling patch antennas by the bond graph approach (Taghouti and Mami, 2011). Then, we apply this method together with the scattering formalism for the electrical modeling of various structures of patch antenna networks. Finally, the validation of the proposed method is performed by a comparative study between the simulations of the scattering parameters  $S_{ij}$  of the studied structure and the simulations of those founded directly from the electrical model of the antenna (Taghouti and Mami, 2012).

## MATERIALS AND METHODS

The new electrical modeling technique, which we have developed since 2009 (Taghouti and Mami, 2009), and which is based on the jointly use of two approaches often namely: the scattering formalism (Paynter *et al.*,

**Corresponding Author:** Hichem Taghouti, Department of Electrical Engineering, Laboratory of Analysis and Control Systems, ENIT-BP 37, 1002 Tunis Le BELVEDERE, Tunisia

This work is licensed under a Creative Commons Attribution 4.0 International License (URL: <http://creativecommons.org/licenses/by/4.0/>).

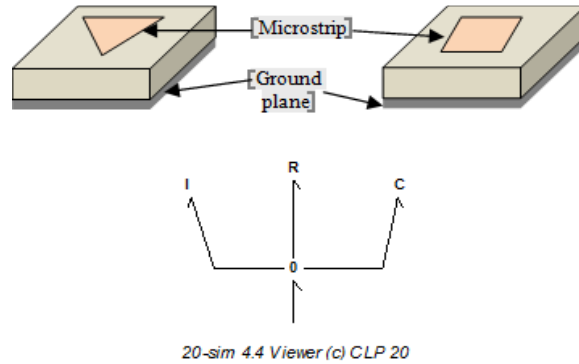


Fig. 1: From patch antenna (triangular and rectangular structure) to bond graph model

1988) and the bond graph approach (Kamel and Dauphin-Tanguy, 1993), provides a quick, simple and effective analysis, and enabling the antenna to integrate with other components. It can be, subsequently, useful if we make changes in the patch and it allows us to, directly, extract the equivalent circuit (Simovski and Sochava, 2003) of the studied patch antenna whatever its geometry (the dimensions of the patch form), the characteristics of the used materials (permittivity, height, thickness and characteristics of the metal's substrate), the nature and position of the excitation so that the set of all losses (Anguera *et al.*, 2009).

**Basic concepts of physical analysis for bond graph modeling of patch antennas:** Generally, the RF and the microwave circuits use three basic lumped element building blocks; capacitors, inductors and resistors (Bahl, 2003). The important advantage of using lumped elements in RF and microwave circuits lies in the fact that several design techniques used in circuits at lower RF frequencies, which are not practical at microwave frequencies using microstrip, coaxial, or waveguide transmission media, can now be successfully applied up to X band frequencies (Sulaiman and Ismail, 2013). An ideal lumped element is not realizable even at lower microwave frequencies because of the associated parasitic reactance due to fringing fields.

At RF and microwave frequencies, each component has associated electric and magnetic fields and finite dissipative loss. Thus, such components store or release electric and magnetic energies across them and their resistance accounts for the dissipated power. The relative values of the  $C$ ,  $L$ , and  $R$  components in these elements depend on the intended use of the lumped elements.

By using the bond graph approach and the previously explication, we can consider that any RF or microwave circuit is a resonant element (Ferchichi *et al.*, 2009) which can be translated to bond graph, generally, by three basic elements namely: resistive element ( $R$ ), inductive element ( $I$ ) and capacitive element ( $C$ ) connected with the junction "0" (Taghouti and Mami, 2009). The determination of these parameters values must include the geometrical parameters of microwave circuit and its environment:

substrate, losses, radiation (Mehouachi *et al.*, 2012; Khmailia *et al.*, 2012).

By referring to the works done by Jmal *et al.* (2013) where the bond graph model of the patch antenna with rectangular or triangular structure is given by the following Fig. 1.

where,

$R$  : Bond graph element (resistive element) modeling the loss of antenna in its environment.

$C$  and  $I$ : The capacitance and inductive elements (Jmal *et al.*, 2013).

**Bond graph models of inductor elements:** In RF and microwave realization, there are three forms (indicated by Fig. 2) of inductors such as: bond-wire and strip sections, circular and rectangular loops, rectangular and circular spirals (Sulaiman and Ismail, 2013; Bahl, 2003).

The tow general bond graph models of those printed inductors are shown in Fig. 3 and 4.

The expressions of inductance  $L$ , resistance  $R_s$  and parasitic capacitance  $C$ ,  $C_1$  and  $C_3$  are given below. These expressions are calculated by *Pr. Inder Bahl* and indicated in his book.

For Microstrip section (Bahl, 2003):

$$L(nH) = 2.10^{-4} \ell \left[ \ln \left( \frac{\ell}{W+t} \right) + 1,193 + \frac{W+t}{3\ell} \right] . K_g \quad (1)$$

$$R_s (\Omega) = \frac{K . R_{sh} \ell}{2.(W+t)} \quad (2)$$

$$C_1 (pF) = 16,67.10^{-4} \ell \sqrt{\frac{\epsilon_{re}}{Z_0}} \quad (3)$$

where,

$K$  : A correction factor

$Z_0$  : Characteristic impedance

$\epsilon_{re}$  : Effective dielectric constant:

$$K_g = 0,57 - 0,145 . \ln \frac{W}{h}, \quad \frac{W}{h} > 0,05 \quad (4)$$

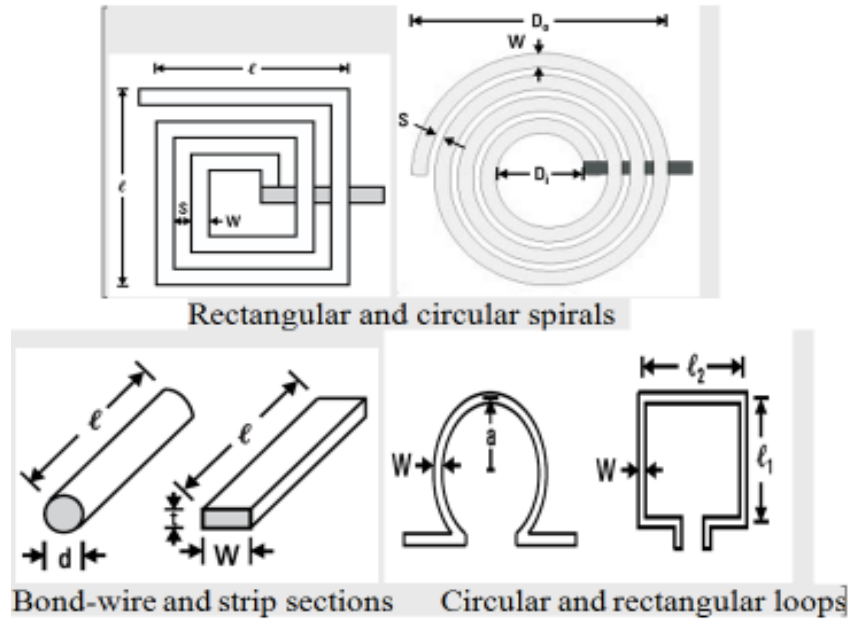


Fig. 2: Inductor configurations

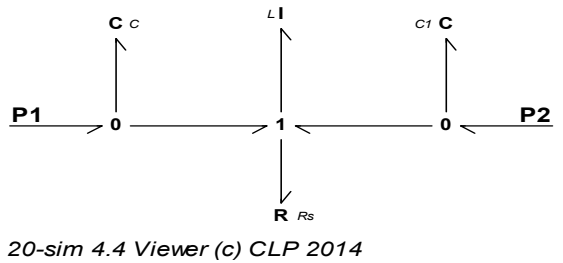


Fig. 3: Bond graph model of microstrip section

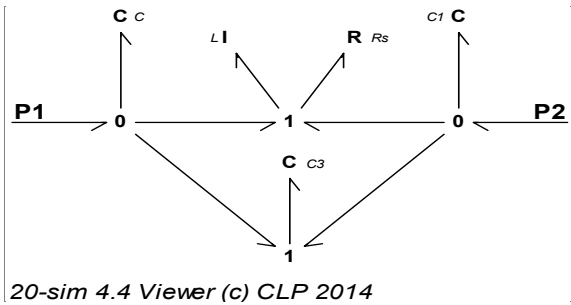


Fig. 4: Bond graph model of circular loops and coils

$$K = 1,4 + 0,217 \cdot \ln\left(\frac{W}{5t}\right) \quad (5)$$

$5\left(\frac{W}{t}\right) < 100$  for a ribbon:

$$K = 1 + 0,333\left(1 + \frac{S}{W}\right) \text{ for a spiral} \quad (6)$$

- For circular loop we have:

$$L(nH) = 1,257 \cdot 10^{-3} a \left[ \ln\left(\frac{a}{W+t}\right) + 0,078 \right] K_g \quad (7)$$

$$R_s(\Omega) = \frac{K \cdot R_{sh}}{(W+t)} \Pi \cdot a \quad (8)$$

$$C_1(pF) = 33,33 \cdot 10^{-4} \Pi \cdot a \sqrt{\frac{\epsilon_{re}}{Z_0}} \quad (9)$$

where, ‘a’ is the mean radius of the Loop

- For circular coil or spiral we have:

$$L(nH) = 0,03937 \frac{a^2 n^2}{8a + 11c} K_g \quad (10)$$

$$R_s(\Omega) = \frac{K \cdot n \cdot R_{sh}}{W} \Pi \cdot a \quad (11)$$

$$C_3(pF) = 3,5 \cdot 10^{-5} D_0 + 0,06 \quad (12)$$

$$a = \frac{D_0 + D_i}{4} \quad (13)$$

$$c = \frac{D_0 - D_i}{2} \quad (14)$$

The terms  $n$ ,  $D_i$ ,  $D_0$ ,  $S$ ,  $a$ ,  $W$ ,  $t$ ,  $h$ ,  $l$  and  $R_{sh}$  are, respectively, the number of turns, inductor’s inside diameter, inductor’s outside diameters, spacing between the turns, the mean radius of the loop, the line width, line thickness, substrate thickness, length of the section

and sheet resistance per square of the conductor (Bahl, 2003).

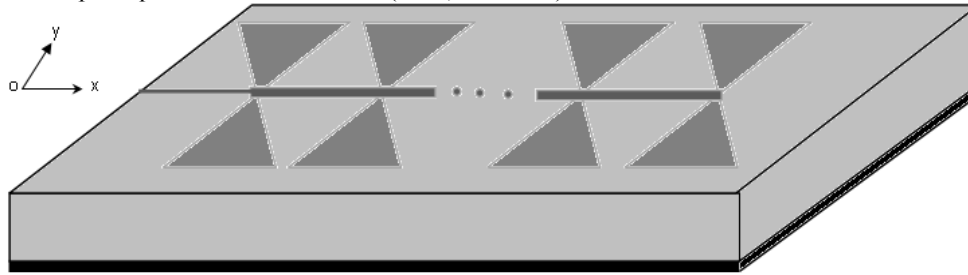


Fig. 5: Antenna array with butterfly geometric structure

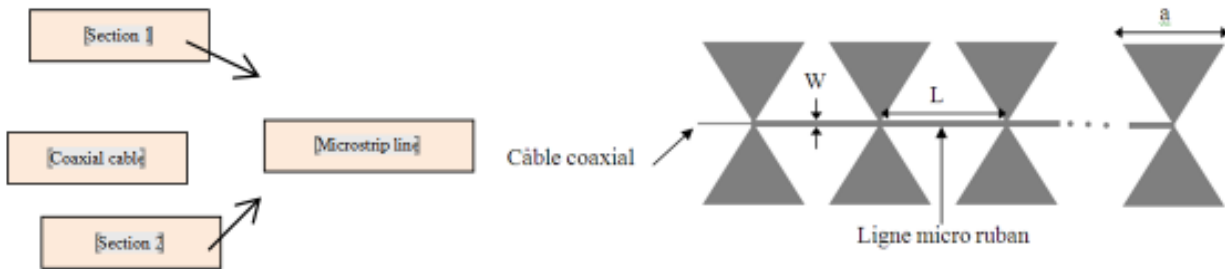


Fig. 6: Antenna array with multi-triangular structure

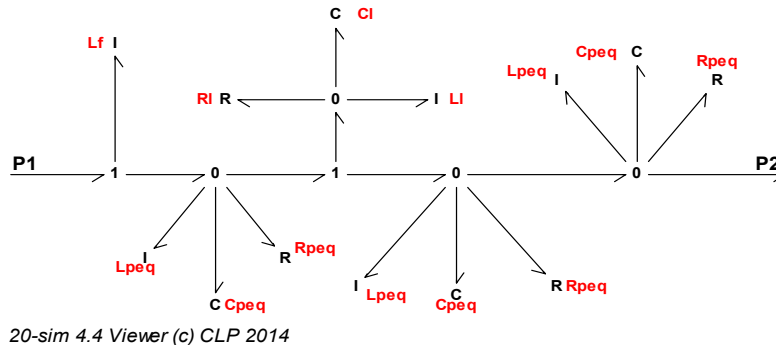


Fig. 7: Compressed bond graph model of antenna array

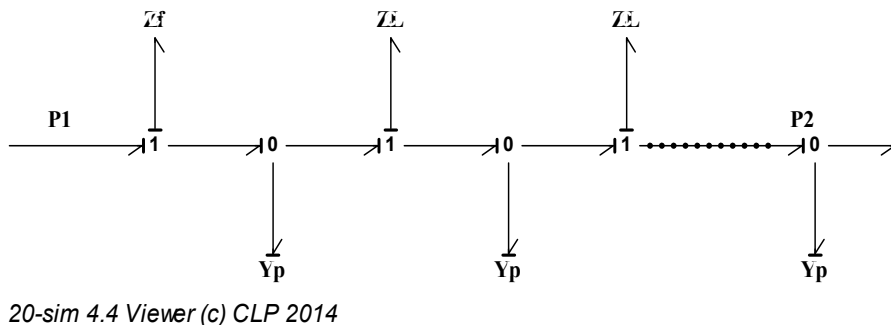


Fig. 8: Reduced and causal bond graph model

## RESULTS AND DESCUSSION

The proposed antenna having a modified butterfly structure connected by a single microstrip line with length  $L$  and width  $W$  is shown in Fig. 5. The structure

is excited by a coaxial cable to the end of the line as shown in Fig. 6.

The top view of the studied structure is shown in Fig. 6. Where,  $a = 3$  mm,  $L = 7$  mm,  $W = 0.15$  mm.

The interconnection between two sections of the antenna is effected via the junction "0", this leads to

the simplified and acausal bond graph model of the multi-triangular antenna array (Taghouti and Mami, 2010) (Fig. 7):

$$\begin{cases} R_{p\acute{e}q} = \frac{R_p}{2} \\ L_{p\acute{e}q} = \frac{L_p}{2} \\ C_{p\acute{e}q} = 2C_p \end{cases} \quad (15)$$

The use of the scattering formalism requires us to transform the bond graph model into a reduced and causal bond graph model to facilitate the determination of the scattering parameters ( $S_{11}$ ,  $S_{12}$ ,  $S_{21}$  and  $S_{22}$ ) of the antenna array (Taghouti *et al.*, 2014) (Fig. 8):

$$\begin{cases} z_f = \tau_{L_f} S \\ y_p = \frac{1}{\tau_{R_{p\acute{e}q}}} + \frac{1}{\tau_{L_{p\acute{e}q}} S} + \tau_{C_{p\acute{e}q}} S \\ y_L = \frac{1}{\tau_{R_l}} + \frac{1}{\tau_{L_l} S} + \tau_{C_l} S \\ z_L = \frac{1}{y_L} \end{cases} \quad (16)$$

$$\begin{cases} \tau_{L_f} = \frac{L_f}{R_0}; \quad \tau_{L_l} = \frac{L_l}{R_0}; \quad \tau_{L_{p\acute{e}q}} = \frac{L_{p\acute{e}q}}{R_0} \\ \tau_{R_{p\acute{e}q}} = \frac{R_{p\acute{e}q}}{R_0}; \quad \tau_{R_l} = \frac{R_l}{R_0} \\ \tau_{C_{p\acute{e}q}} = C_{p\acute{e}q} R_0; \quad \tau_{C_l} = C_l R_0 \end{cases} \quad (17)$$

The breakdown (decomposition), presented by Fig. 9, of the previous bond graph model is important. Just insert junctions ‘1’ between the cells [0-1] or [1-0] to have same causal and reduced sub-models, from which we can find the wave matrices  $W$ , then the scattering matrices  $S$  (Taghouti *et al.*, 2012). The tow bond graph sub-models are given by the Fig. 10.

After decomposing the complex BG model in the form of [0-1] or [1-0] cells, we use the analytical method of operating scattering parameters (Mehouachi

*et al.*, 2014; Taghouti and Mami, 2011), which consist to put each cell as an intervening process between two input and output ports as shown in the following Fig. 11.

From each cell, by taking into account the type of assignment of causality, we determine the causal loops and paths and the Integro-differential operators  $H_{ij}$  of the cell:

$$B_i = \frac{-1}{Z_L Y_p} : \text{Gain of causal loop of one BG cell}$$

$$\Delta_i = 1 + \frac{1}{B_i} : \text{Determinant of one causal BG cell}$$

The Integro-differential operators of one BG cell with effort-flux causality are given bellow:

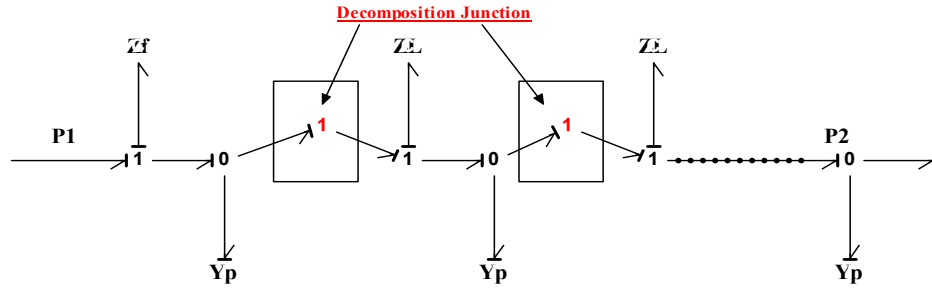
$$\begin{cases} H_{11} = \frac{Z_L}{B_i + 1} \\ H_{12} = \frac{1}{B_i + 1} \\ H_{21} = \frac{1}{B_i + 1} \\ H_{22} = \frac{-Y_p}{B_i + 1} \\ \Delta H = \frac{-1}{B_i + 1} \end{cases} \quad (18)$$

These operators can lead us to the wave matrix  $W_i$  of each BG cell:

$$W_i = \frac{1}{2} \begin{bmatrix} z_L y_p + z_L + y_p + 2 & z_L y_p - z_L + y_p \\ z_L y_p + z_L - y_p & z_L y_p - z_L - y_p + 2 \end{bmatrix} \quad (19)$$

The global wave matrix  $W_g$  is given bellow, where  $N$  is the number of BG cell:

$$W_g = \prod_{i=1}^N W_i = \begin{bmatrix} W_{11} & W_{12} \\ W_{21} & W_{22} \end{bmatrix} \quad (20)$$



20-sim 4.4 Viewer (c) CLP 2014

Fig. 9: Decomposed bond graph model

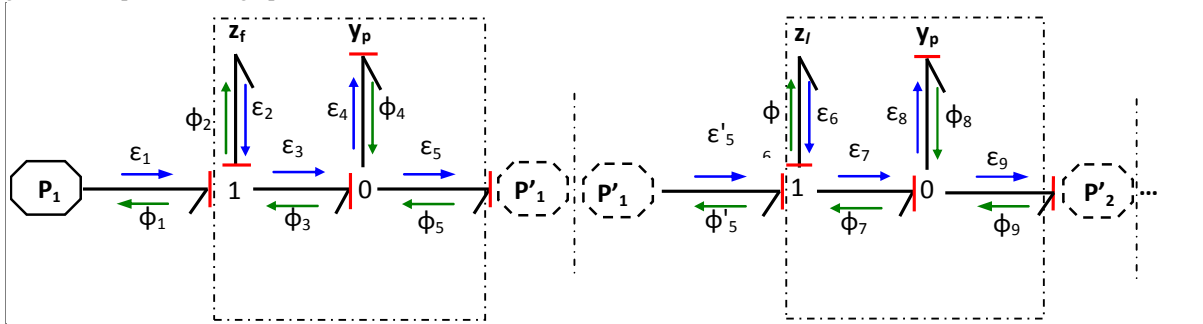


Fig. 10: Bond graph cells of the multi-triangular antenna array



Fig. 11: Bond graph model with the effort-flux causality

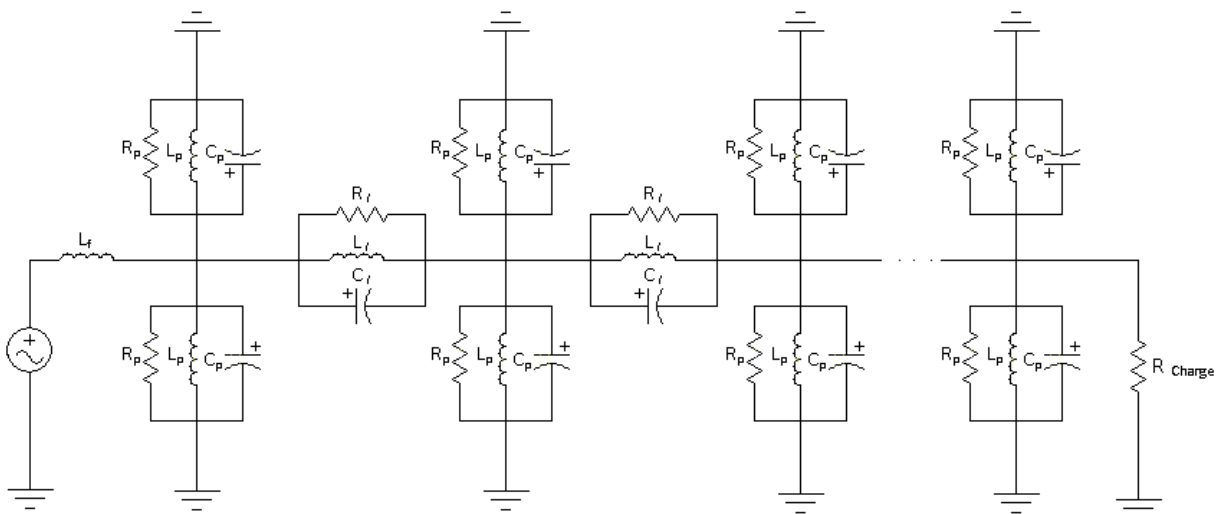


Fig. 12: Equivalent circuit of the multi-triangular patch antenna array

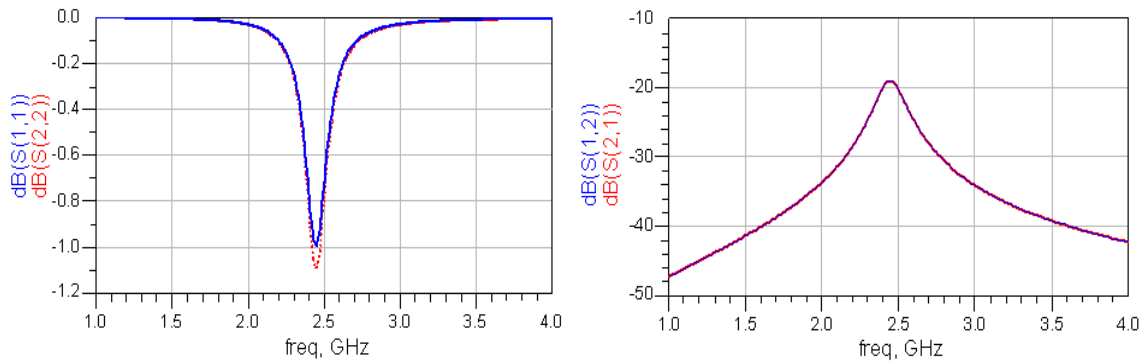


Fig. 13: EC's reflexion and transmission coefficients  $S_{ij}$  Simulation (with six multi-triangular sections)

By the same method, we easily exploiting the scattering matrix  $S_{ij}$  of the overall system (bond graph model):

$$S_{ij} = \begin{bmatrix} W_{12}W_{22}^{-1} & [W_{11}W_{22} - W_{21}W_{12}]W_{22}^{-1} \\ W_{22}^{-1} & -W_{21}W_{22}^{-1} \end{bmatrix} \quad (21)$$

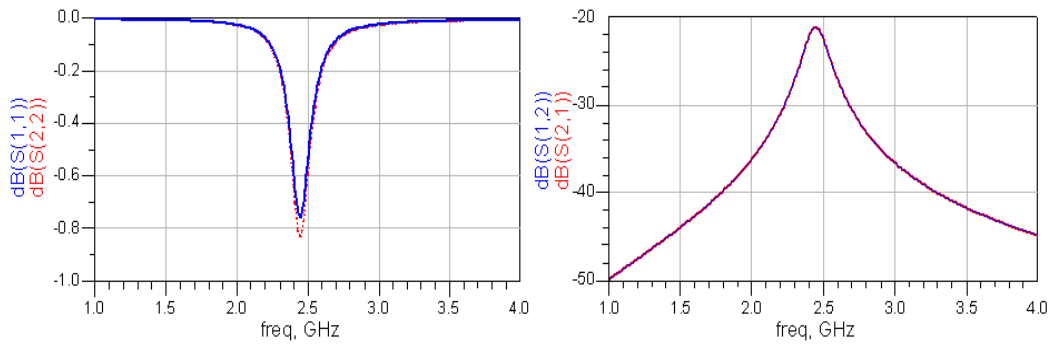


Fig. 14: EC's reflexion and transmission coefficients  $S_{ij}$  Simulation (with eight multi-triangular sections)

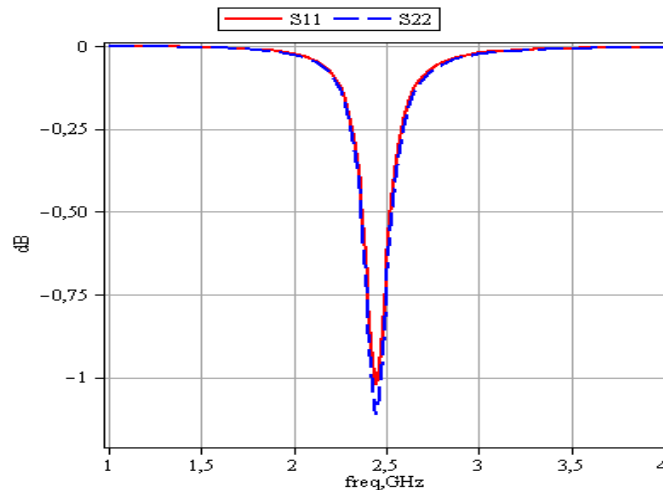


Fig. 15: Reflexion coefficients  $S_{11}$  and  $S_{22}$  from bond graph model of six multi-triangular sections

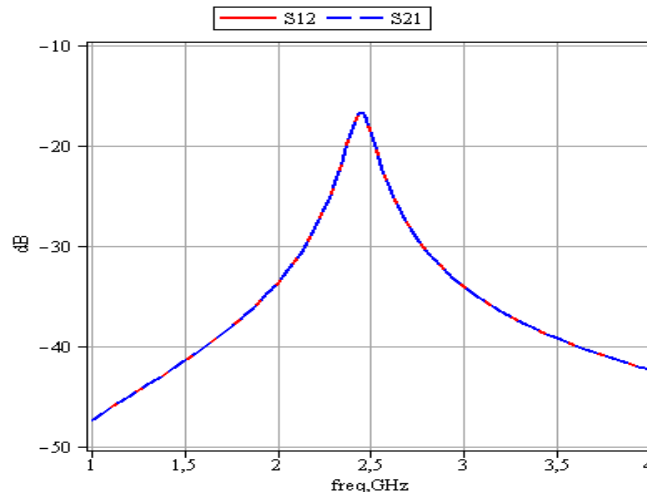


Fig. 16: Reflexion coefficients  $S_{12}$  and  $S_{21}$  from bond graph model of six multi-triangular sections

We simulate the scattering parameters  $S_{ij}$ , respectively, by six and eight multi-triangular sections.

**Extraction and simulation of the equivalent circuit from the bond graph model:** By using the bond graph model of Fig. 7 and by referring to the previously

papers (Mehouachi *et al.*, 2014), we can extract, directly, the Equivalent Circuit (EC) of the multi-triangular antenna array (Fig. 12).

The simulation of the scattering parameters extracted from the EC of patch antenna, gives us the Fig. 13 and 14. The comparison between these results

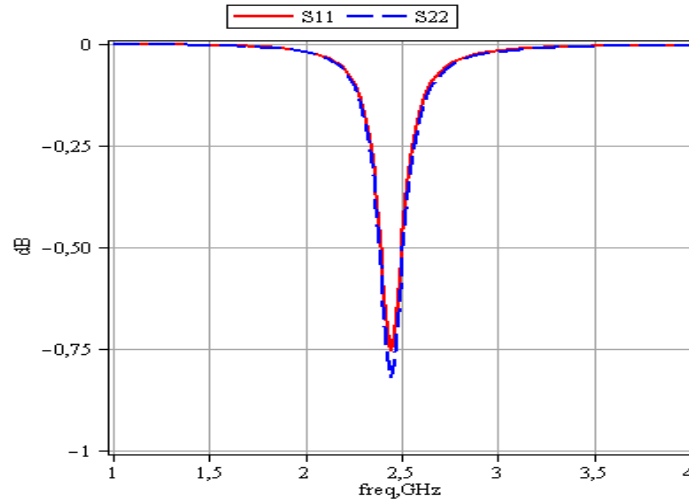


Fig. 17: Reflexion coefficients  $S_{11}$  and  $S_{22}$  from bond graph model of eight multi-triangular sections



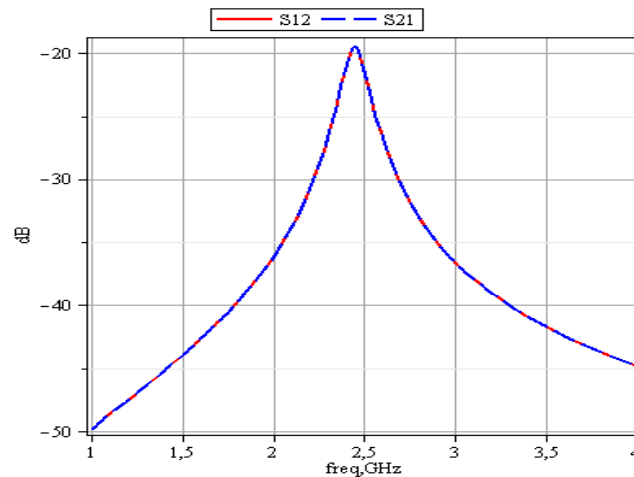


Fig. 18: Reflexion coefficients  $S_{12}$  and  $S_{21}$  from bond graph model of six multi-triangular sections

and the others (Fig. 15 to 18), confirm us the best choice of our new electrical modeling technique.

### CONCLUSION

In this study, we have applied our own method of analysis for the electrical modeling and simulation of antenna patch structures with complex geometry such as multi-triangular antenna networks. This method is based on the joint use of the bond graph approach and the scattering formalism; it is easy to handle, easy for non-specialists, reliable and very fast.

### ACKNOWLEDGMENT

The authors would like to acknowledge especially Prof. MAMI Abdelkader for the time and guidance given throughout the all carried out works, without forgetting the members of the unit of electronics and high frequency circuits and all those who contributed and aided for this study in particularly LACS members (Laboratory of analysis and command systems).

### REFERENCES

Anguera, J., C. Puente and C. Borja, 2009. Dual frequency broadband microstrip antenna with a reactive loading and stacked elements. *Prog. Electromagn. Res. Lett.*, 1(10):1-10.

Bahl, I.J., 2003. *Lumped Elements for RF and Microwave Circuits*. Artech House, Norwood, MA.

Ferchichi, A., N. Fadlallah, N. Sboui and A. Gharssalah, 2009. Analysis and design of printed fractal antennas by using an adequate electrical model. *Int. J. Commun. Network. Inform. Secur.*, 1(3): 65-69.

Galehdar, A., D.V. Thiel and S.G. O'Keefe, 2007. Antenna efficiency calculations for electrically

small, RFID antennas. *IEEE Antenn. Wirel. Pr.*, 6: 156-159.

Jmal, S., H. Taghouti and A. Mami, 2013. A new modeling and simulation methodology of a patch antenna by bond graph approach. *Proceeding of the IEEE International Conference on Electrical Engineering and Software Applications (ICEESA)*, pp: 1-6.

Kamel, A. and G. Dauphin-Tanguy, 1993. Bond graph modeling of power waves in the scattering formalism. *J. Simulat. Ser.*, 25: 41-41.

Khmailia, S., H. Taghouti, R. Mehouchi and A. Mami, 2012. Analyze of a rectangular microstrip antenna by the scattering bond graph approach. *Int. J. Elect. Com. Eng. Tech. (IJECET)*, 3(1).

Mehouchi, R., H. Taghouti, S. Khmailia and A. Mami, 2012. Modelling and determination of the scattering parameters of wideband patch antenna by using a bond graph approach. *Int. J. Eng. Res. App.*, 2(5): 879-884.

Mehouchi, R., H. Taghouti and A. Mami, 2014. Analysis of microstrip patches antennas array by using a new bond graph technology. *Am. J. Appl. Sci.*, 11(8): 1436-1449.

Mekki, M., 2004. Evaluation des méthodes appliquées à l'analyse électromagnétique des systèmes radioélectriques très hautes fréquences embarqués dans l'environnement automobile. Application: Radar anticollision à 76GHz. Ph.D. Thèse, Université Paris 6.

Paynter, H.M., J. Ilene and Busch-Vishniac, 1988. Wave scattering approaches to conservation and causality. *J. Frankl. Inst.*, 325(3): 295-313.

Pozart, D.M., 1998. *Microwave Engineering*. 2nd Edn., John Wiley Sons, New York.

Simovski, C.R. and A.A. Sochava, 2003. High-impedance surfaces based on self-resonant grids. *Analytical modelling and numerical simulations. Prog. Electromagn. Res.*, 43: 239-256.

- Su, Z., Y. Liu, W. Yu and R. Mittra, 2004. A conformal mesh-generating technique for the conformal finite-difference time-domain (CFDTD) method. *IEEE Antennas Propag.*, 46(1): 37-49.
- Sulaiman, N.H. and M.Y. Ismail, 2013. Dual frequency X-band reflect array antenna using dual gap. *Proc. Eng.*, 53: 271-277.
- Taghouti, H. and A. Mami, 2009. Application of the reduced bond graph approaches to determinate the scattering parameters of high frequency filter. *Proceeding of the 10th International Conference on Science and Techniques of Automatic Control and Computer Engineering. Tunisia*, pp: 379-391.
- Taghouti, H. and A. Mami, 2010. How to find wave-scattering parameters from the causal bond graph model of a high frequency filter. *Am. J. Appl. Sci.*, 7(5): 702-710.
- Taghouti, H. and A. Mami, 2011. New extraction method of the scattering parameters of a physical system starting from its causal bond graph model: Application to a microwave filter. *Int. J. Phys. Sci.*, 6(13): 3016-3030.
- Taghouti, H. and A. Mami, 2012. Discussion around the scattering matrix realization of a microwave filter using the bond graph approach and scattering formalism. *Am. J. Appl. Sci.*, 9(4): 459-467.
- Taghouti, H., S. Khmailia, R. Mehouchi and A. Mami, 2012. Using of a new bond graph technology for the study of a high frequency low pass filter. *Int. J. Comput. Eng. Manage.*, 15(5): 9-15.
- Taghouti, H., A. Mami and S. Jmal, 2014. *Nouvelle Technique de Modélisation et Simulation par Bond Graph: Applications aux Circuits Hauts Fréquences et Antennes Patch*. Saarbrücken Éditions Universitaires Européennes (13 février 2014). ISBN-10: 3841730582; ISBN 13: 978-3841730589.